Available online at www.sciencedirect.com
SCIENCE DIRECT®
Advances in Space Research 36 (2005) 846–854
ADVANCES IN SPACE RESEARCH (a COSPAR publication)
www.elsevier.com/locate/asr

NO_2 and BrO vertical profile retrieval from SCIAMACHY limb measurements: Sensitivity studies

A. Rozanov [a,*], H. Bovensmann [a], A. Bracher [a], S. Hrechanyy [b], V. Rozanov [a], M. Sinnhuber [a], F. Stroh [b], J.P. Burrows [a]

[a] Institute of Environmental Physics/Institute of Remote Sensing, University of Bremen, FB 1, Otto-Hahn-Allee 1, 28359 Bremen, Germany
[b] Institute for Stratospheric Chemistry, Research Centre Jülich (FZJ), 52425 Jülich, Germany

Received 1 October 2004; received in revised form 11 February 2005; accepted 3 March 2005

Abstract

A retrieval algorithm used to obtain vertical distributions of NO_2 and BrO from SCIAMACHY limb measurements is described. Furthermore, the information content of SCIAMACHY limb measurements with respect to NO_2 and BrO profile retrievals is investigated. Another investigated aspect is a sensitivity of resulting NO_2 and BrO vertical profiles to a priori trace gas vertical distributions as well as to the pressure and temperature profiles used in the forward modeling. The sensitivity region is estimated to be 12–40 km for NO_2 and 12–35 km for BrO. Larger retrieval errors are encountered below 15 km associated to the influence of the neighboring altitude levels and of a priori information. The dependence of the retrieved trace gas vertical distributions on the pressure and temperature profiles used in the forward model is found to be insignificant above 20 km, whereas it cannot be completely ignored when retrieving trace gas amounts below.

Keywords: SCIAMACHY; Vertical profile retrieval; Limb measurements; Sensitivity

1. Introduction

The Scanning Imaging Absorption Spectrometer for Atmospheric Chartography (SCIAMACHY) launched on board the European Environment Satellite (ENVISAT-1) in March 2002 is one of the newest space-borne instruments intended to improve our knowledge of the atmospheric physics and chemistry. The SCIAMACHY instrument measures the scattered and reflected spectral radiance in nadir and limb geometry and the spectral radiance transmitted through the atmosphere in solar/lunar occultation geometry in the spectral region 240–2380 nm. A detailed description of the instrument design and capabilities is given by Bovensmann et al. (1999) and the first results of in-flight performance are presented by Bovensmann et al. (2004).

First retrievals of SCIAMACHY measurements in limb viewing geometry demonstrate a huge information content of the measured data. For example, vertical distributions of atmospheric trace gases retrieved from SCIAMACHY limb measurements were used by von Savigny et al. (2005) to investigate the ozone hole split over Antarctic during the major stratospheric warming in September 2002. Despite remaining problems due to imperfect data calibration and pointing knowledge (Kaiser et al., 2004), newly developed retrieval algorithms were shown to provide vertical distributions of such atmospheric trace gases as ozone, NO_2, and BrO with a reasonable accuracy.

Whereas NO_2 vertical profiles were previously successfully retrieved from limb scattering measurements performed by such instruments as SME (Mount et al.,

* Corresponding author. Tel.: +49 421 2184584; fax: +49 421 2184555.
E-mail address: alex@iup.physik.uni-bremen.de (A. Rozanov).

0273-1177/$30 © 2005 COSPAR. Published by Elsevier Ltd. All rights reserved.
doi:10.1016/j.asr.2005.03.013

1984) and OSIRIS (Sioris et al., 2003; Haley et al., 2004), SCIAMACHY is the first limb-viewing instrument enabling the vertical distributions of BrO to be retrieved from the measurements of the scattered solar radiation.

For a future utilization of the retrieved vertical distributions of atmospheric species a sensitivity of the measurements needs to be investigated. This will provide an information on the origin of the retrieved trace gas amounts in different altitude regions, i.e., whether the retrieved amount at a particular altitude is determined by the real state of the atmosphere or originated from a priori information used in the forward model and/or in the retrieval algorithm. This can be done by analyzing the averaging kernels (Rodgers, 2000) and the weighting functions (see below) specific to the measurements geometry and to the employed retrieval procedure.

Actual accuracy of the retrieval can only be estimated comparing a statistically significant amount of the retrieved profiles to the results obtained by other instruments. However, for minor trace gases like NO_2 and BrO almost no directly comparable measurements are available and any kind of conversion introduces additional uncertainties complicating an estimation of the real accuracy of the retrieved profiles. In this case, the reliability of the retrieval can be estimated looking at the theoretical precisions (Rodgers, 2000) and analyzing the dependence of the retrieved profiles on input parameters of the forward model and the retrieval procedure.

In the scope of this paper a retrieval algorithm employed to obtain vertical distributions of NO_2 and BrO from SCIAMACHY limb measurements is described. Sensitivity of the retrieval in different altitude regions is discussed and the dependence of the retrieved profiles on a priori trace gas vertical distributions and vertical profiles of pressure and temperature is investigated.

2. Retrieval algorithm

Measurements of the scattered solar radiation in limb viewing geometry as performed by the SCIAMACHY instrument are simulated using the CDI radiative transfer model (Rozanov et al., 2001). The model calculates the limb radiance properly considering the single scattered radiance and using an approximation to account for the multiple scattering. The CDI radiative transfer model is linearized with respect to the absorption coefficient, i.e., it can be used to calculate weighting functions of atmospheric trace gases needed by the retrieval procedure to evaluate the vertical distributions. The radiance and weighting functions simulated with CDI model were compared to the results of other radiative transfer models demonstrating a good agreement at viewing geometries specific to SCIAMACHY limb measurements (Loughman et al., 2004; Postylyakov, 2004).

The weighting function at a particular wavelength, λ, is defined as a variation of the outgoing radiance at this wavelength, $I(\lambda)$, due to a variation in the vertical distribution of the trace gas of interest, α, at a certain altitude level, z_i. For limb measurements the dependence of the outgoing radiance and, therefore, of the weighting functions on the tangent height, h_j, is essential:

$$W_j(\lambda, z_i) = \frac{\delta I_j(\lambda)}{\delta \alpha(z_i)} \alpha(z_i), \quad j = 1, \ldots, N_{\text{th}}, \quad i = 1, \ldots, N_z. \tag{1}$$

Here, N_{th} is the total number of tangent heights and N_z is the total number of altitude levels.

For NO_2 vertical profile retrieval, the outgoing radiance and the weighting functions are computed at tangent heights between 12 and 46 km in the spectral range from 420 to 490 nm. Beside NO_2, the weighting functions of ozone are employed. In the case of BrO, the calculations are performed at tangent heights between 12 and 38 km in the spectral window from 335 to 360 nm. The weighting functions of BrO, ozone, NO_2, and O_4 are used in the retrieval procedure. The retrieval is performed using ratios of limb spectra in a selected tangent height range to the reference spectrum. The limb measurements at tangent heights of about 46 km and of about 38 km are used as reference spectra for NO_2 and BrO vertical profile retrievals, respectively.

The retrieval algorithm consist of two steps, namely, the preprocessing step aimed to get rid of spectral features not associated to the retrieved parameters and the main inversion procedure.

At the preprocessing step, the ratios of limb spectra at different tangent heights to the measurement at a reference tangent height are treated independently one by one. At each tangent height, a polynomial of an appropriate order (cubic polynomial for NO_2 and BrO retrievals) is subtracted from the logarithms: (i) of measured limb radiance at this tangent height, $I_j^{\text{m}}(\lambda)$, (ii) of measured limb radiance at the reference tangent height (reference spectrum), $I_{\text{ref}}^{\text{m}}(\lambda)$, and (iii) of simulated ratio spectrum, $R_j^{\text{s}}(\lambda)$, (i.e., ratio of modeled limb spectra at current and reference tangent heights, $I_j^{\text{s}}(\lambda)$ and $I_{\text{ref}}^{\text{s}}(\lambda)$, respectively) as well as from logarithmic weighting functions in order to account for unknown scattering characteristics of the atmosphere and broadband instrument calibration errors. Resulting functions are denoted as differential spectra, $\tilde{I}_j^{\text{m}}$, $\tilde{I}_{\text{ref}}^{\text{m}}$, and $\tilde{R}_j^{\text{s}}$, (measured, reference, and simulated ratio, correspondingly) and differential weighting functions $\tilde{W}_j$:

$$\tilde{I}_j^{\text{m}}(\lambda) = \ln[I_j^{\text{m}}(\lambda)] - \sum_{i=0}^{N} a_i^{\text{m},j} \lambda^i, \tag{2}$$

$$\tilde{I}^{\mathrm{m}}_{\mathrm{ref}}(\lambda) = \ln[I^{\mathrm{m}}_{\mathrm{ref}}(\lambda)] - \sum_{i=0}^{N} a_i^{\mathrm{m,ref}} \lambda^i, \tag{3}$$

$$\tilde{R}^{\mathrm{s}}_j(\lambda) = \ln\left[\frac{I^{\mathrm{s}}_j(\lambda)}{I^{\mathrm{s}}_{\mathrm{ref}}(\lambda)}\right] - \sum_{i=0}^{N} a_i^{\mathrm{s},j} \lambda^i, \tag{4}$$

$$\tilde{W}^k_j(\lambda) = \frac{W^k_j(\lambda)}{I^{\mathrm{s}}_j(\lambda)} - \frac{W^k_{\mathrm{ref}}(\lambda)}{I^{\mathrm{s}}_{\mathrm{ref}}(\lambda)} - \sum_{i=0}^{N} a_i^{k,j} \lambda^i, \quad k = 1, \ldots, N_{\mathrm{tg}}. \tag{5}$$

Here, j denotes the tangent height index, k is the retrieval parameter index, N_{tg} is the total number of atmospheric trace gases to be retrieved, and N is a polynomial order. The weighting functions employed here are vertically integrated, i.e., they represent a change of the differential limb radiance due to a scaling of a trace gas vertical profile.

Further in the course of the preprocessing step, a shift and squeeze correction as well as scaling factors for available correction spectra (e.g., ring spectrum, undersampling, stray light correction, etc.) are determined at each tangent height minimizing the following quadratic form:

$$\left\| \tilde{I}^{\mathrm{m}}_j(\lambda) - \tilde{I}^{\mathrm{m}}_{\mathrm{ref}}(\lambda) - \tilde{R}^{\mathrm{s}}_j(\lambda) - \sum_k s_k \tilde{W}^k_j(\lambda) - \sum_l c^l_{\mathrm{sc}} S_l(\lambda) - (c^{\mathrm{s}}_{\mathrm{shi}} - c^{\mathrm{s}}_{\mathrm{sq}}\lambda)\frac{\mathrm{d}R^{\mathrm{s}}_j(\lambda)}{\mathrm{d}\lambda} - (c^{\mathrm{ref}}_{\mathrm{shi}} - c^{\mathrm{ref}}_{\mathrm{sq}}\lambda)\frac{\mathrm{d}\tilde{I}^{\mathrm{m}}_{\mathrm{ref}}(\lambda)}{\mathrm{d}\lambda} \right\|^2 \to \min. \tag{6}$$

Here, s_k are scaling factors for atmospheric trace gas profiles, i.e., $\delta\alpha_k(z_i) = s_k\alpha_k(z_i)$, and c^l_{sc} are scaling factors for the correction spectra, $S_l(\lambda)$. Shift and squeeze correction is done for the ratio of the modeled spectra with respect to the measured spectrum, represented by the coefficients $c^{\mathrm{s}}_{\mathrm{shi}}$ and $c^{\mathrm{s}}_{\mathrm{sq}}$, correspondingly, as well as for the limb measurement at the reference tangent height with respect to the measurement at current tangent height, represented by $c^{\mathrm{ref}}_{\mathrm{shi}}$ and $c^{\mathrm{ref}}_{\mathrm{sq}}$. All coefficients here are tangent height dependent, subscript j is omitted for simplicity.

At the inversion step, vertical profiles of atmospheric trace gases are retrieved solving the following equation:

$$\mathbf{y} = \mathbf{K}\mathbf{x} + \epsilon, \tag{7}$$

where ϵ denotes errors of any kind, e.g., measurement noise, linearization error, and so on. The measurement vector, $\boldsymbol{y}$, contains the differences between ratios of simulated and measured differential limb spectra for all spectral points within the selected spectral intervals at all selected tangent heights with all corrections from the preprocessing step, except trace gas profiles scaling, applied, i.e.,

$$\mathbf{y} = [y_1(\lambda_1), \ldots, y_1(\lambda_{N_{\mathrm{wl}}}), \ldots, y_{N_{\mathrm{th}}}(\lambda_1), \ldots, y_{N_{\mathrm{th}}}(\lambda_{N_{\mathrm{wl}}})], \tag{8}$$

where N_{wl} is the total number of the spectral points in the selected spectral region and N_{th} is the total number of the selected tangent heights. The state vector, $\boldsymbol{x}$, contains relative differences of trace gas number densities (with respect to initial values) at all altitude layers for all gases to be retrieved, i.e.,

$$\mathbf{x} = [x_1(h_1), \ldots, x_1(h_{N_{\mathrm{h}}}), \ldots, x_{N_{\mathrm{tg}}}(h_1), \ldots, x_{N_{\mathrm{tg}}}(h_{N_{\mathrm{h}}})], \tag{9}$$

where N_{h} is the total number of layers in the retrieval altitude grid and N_{tg} is the total number of atmospheric trace gases to be retrieved. The linearized forward model operator, $\boldsymbol{K}$, is represented by a matrix having $N_{\mathrm{wl}} \times N_{\mathrm{th}}$ rows and $N_{\mathrm{h}} \times N_{\mathrm{tg}}$ columns containing corresponding differential weighting functions, $\tilde{W}$.

Solution of Eq. (7) is found employing either the optimal estimation method (Rodgers, 2000) or the information operator approach (Hoogen et al., 1999).

The final solution is found iteratively subsequently running the forward model and the retrieval procedure. The trace gas vertical profiles retrieved in the previous iteration are used as a priori information at each particular iterative step.

The retrieval is performed employing all available spectral points between 420 and 490 nm for NO_2 and between 337 and 357 nm for BrO. Fig. 1 shows examples of spectral fits in NO_2 spectral window at a tangent height of 28 km and in BrO spectral window at a tangent height of 18 km. In order to highlight the spectral signature of BrO, absorption features of other atmospheric species were removed in the spectral fit for BrO shown in the right plot. The corresponding measurements were performed on August 28th, 2002 at 53°N,3°W.

Stratospheric NO_2 profiles can be retrieved in the altitude range from about 15 up to 35–40 km. The retrieval is performed taking into account NO_2 and ozone absorption. Besides shift and squeeze only a stray light correction is done for NO_2 at the preprocessing step which in the case of wavelength independent stray light is represented by the inverse radiance at the reference tangent height. The accuracy of the retrieved number densities is estimated to be about 15–20% between 15 and 30 km. Above 30 km, and in situations of lower stratospheric NO_2 amounts larger errors may occur. Fig. 2 shows a comparison of the NO_2 vertical profiles retrieved from SCIAMACHY limb measurements performed on August 28th, 2002 with HALOE (Russel et al., 1993) and SAGE II (Mauldin et al., 1985) results. Since both HALOE and SAGE II instruments measure the solar light transmitted through the Earth's atmosphere at local sunrise or sunset, the difference between the local solar zenith angles must be taken into account when comparing the NO_2 vertical profiles obtained from these instruments to the SCIAMACHY results. This is

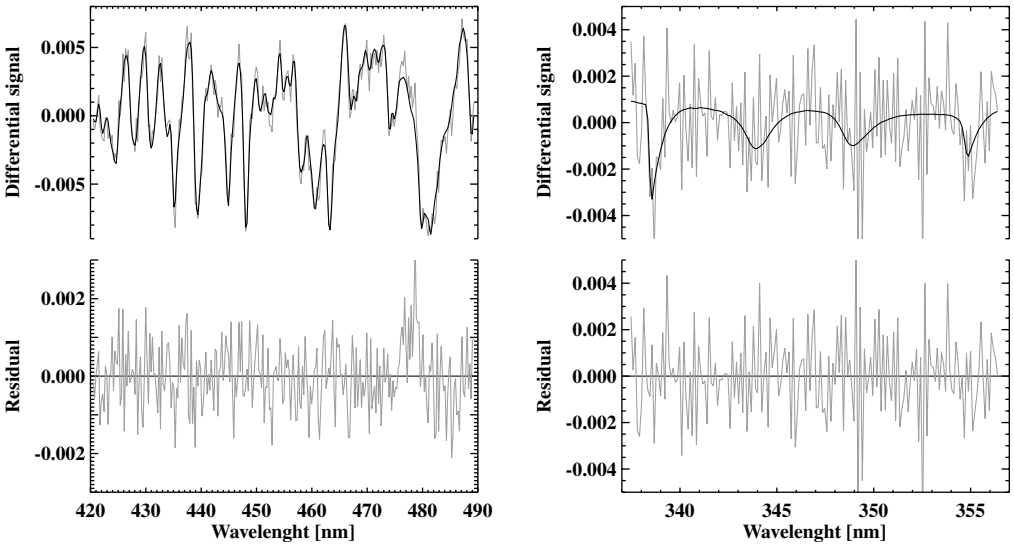

Fig. 1. Examples of spectral fits in NO_2 spectral window at a tangent height of 28 km (left plot) and in BrO spectral window at a tangent height of 18 km (right plot). The upper plots show the measured (grey line) and the simulated (black line) differential signals and the lower plots show the residuals. The corresponding measurements were performed on August 28th, 2002 at 53°N,3°W.

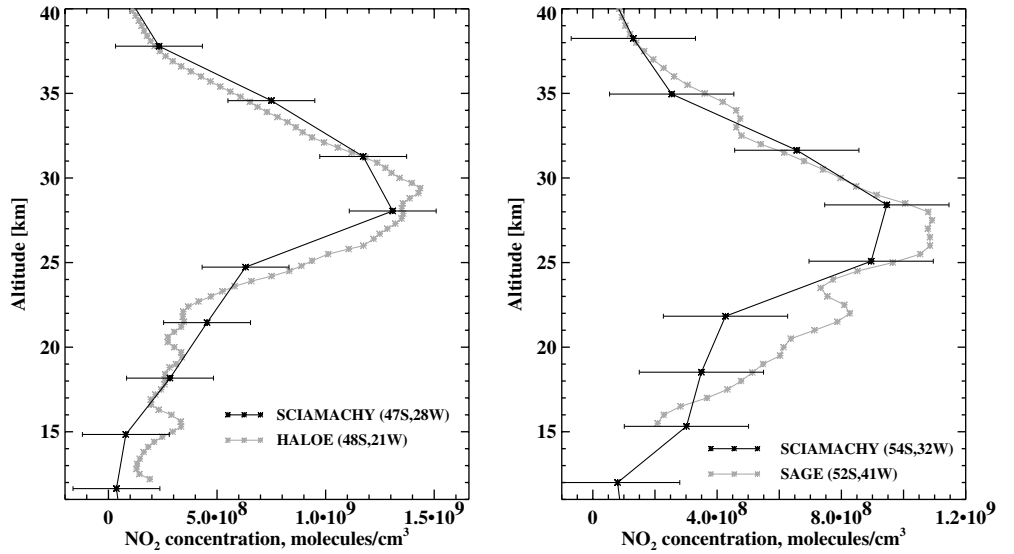

Fig. 2. Comparison of the NO_2 vertical profiles retrieved from SCIAMACHY limb measurements to the results from HALOE (left plot) and SAGE II (right plot).

done transforming the NO_2 vertical profiles measured by HALOE and SAGE II to the solar zenith angle appropriate to the corresponding SCIAMACHY measurement employing a one-dimensional photochemical model. The comparison procedure is discussed in more detail by Bracher et al. (2005). As clearly seen, the NO_2 vertical profiles retrieved from SCIAMACHY limb measurements are in good overall agreement with the results from other instruments.

Vertical profiles of BrO can be retrieved in the altitude range from approximately 14–15 km to about 30 km. Besides BrO, the absorption by ozone, NO_2 and O_4 is taken into account in the retrieval procedure. Additional to shift and squeeze correction a differential Ring spectrum (i.e., ratio of simulated Ring spectra with a polynomial subtracted) is used at the preprocessing step for BrO. The retrieval accuracy is estimated to be about 30–40%. Fig. 3 shows a comparison of the BrO vertical profiles retrieved from SCIAMACHY limb measurements performed on September 24th, 2002 and on June 9th, 2003 with profiles obtained by the TRIPLE instrument performing balloon-borne in situ measurements. As seen from the plot, on September 24th, 2002 the SCIAMACHY instrument detects larger amount of BrO compared to TRIPLE whereas a perfect agreement takes place on June 9th, 2003. The number density profiles retrieved from SCIAMACHY limb measurements were converted to volume mixing ratios using

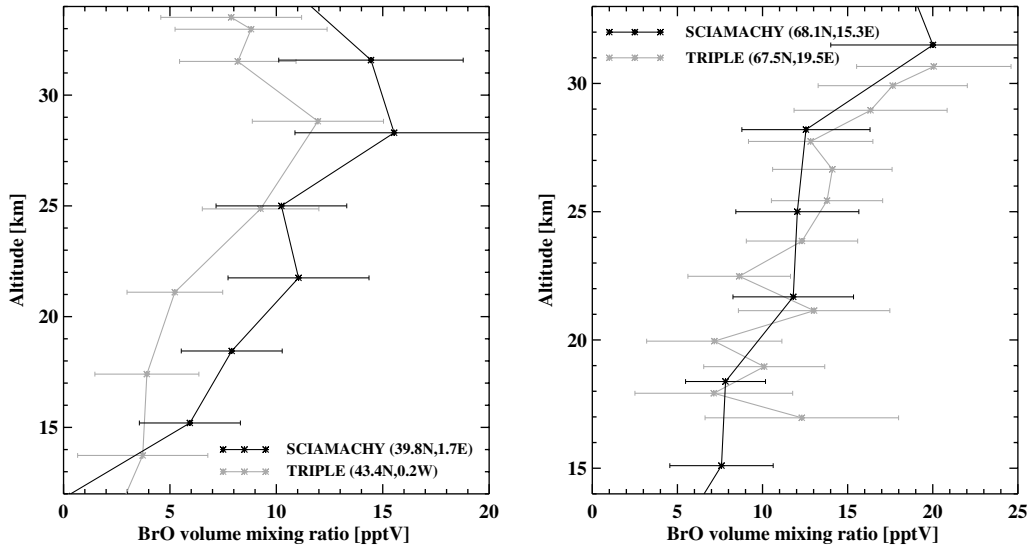

Fig. 3. Comparison of the BrO vertical profiles retrieved from SCIAMACHY limb measurements to the profiles measured by the TRIPLE instrument on September 24th, 2002 (left plot) and on June 9th, 2003 (right plot).

pressure and temperature profiles measured by the TRIPLE instrument. Since both measurements were performed during the daytime no photochemical correction was applied.

3. Sensitivity studies

All results presented in this section were obtained employing the optimal estimation method. A priori covariance matrix was represented by a diagonal matrix with diagonal elements corresponding to 100% a priori uncertainty. The measurement error covariance matrix was also diagonal with diagonal elements corresponding to a wavelength independent signal to noise ratio of 2000.

Fig. 4 shows the theoretical precision (left plot), averaging kernels (middle plot), and differential weighting functions at 439.4 nm (right plot) for NO_2 vertical profile retrieval from SCIAMACHY limb measurements. The results were obtained using the limb measurement at a tangent height of 41.5 km as a reference spectrum. The theoretical precision of the retrieval is about 5% in the altitude region 20–32 km decreasing to 10–20% above 32 km and between 15 and 20 km. Below 15 km the theoretical precision degrades to more than 70% indicating that retrieval results in this altitude region are strongly affected by a priori information. A similar

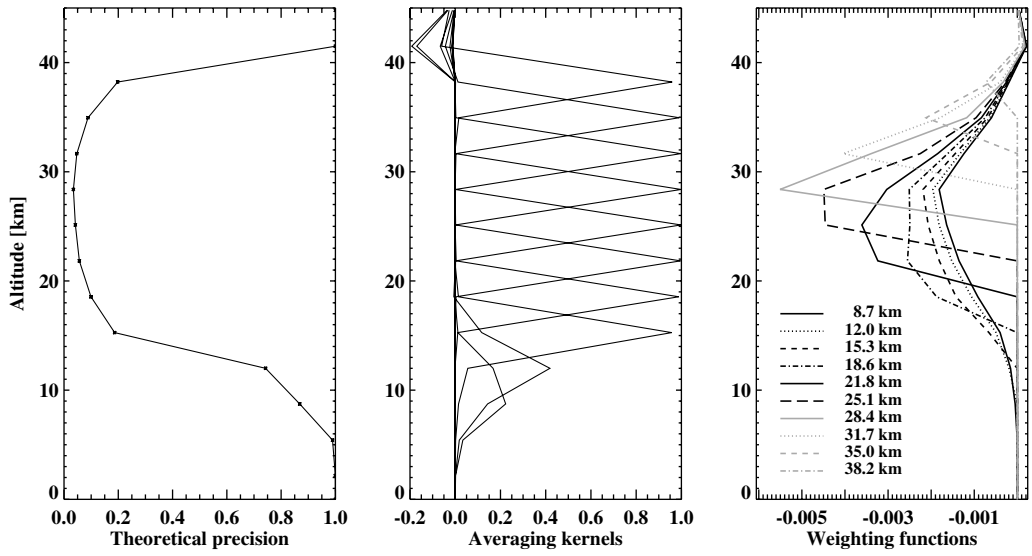

Fig. 4. Theoretical precision (left plot), averaging kernels (middle plot), and differential weighting functions at 439.4 nm (right plot) for NO_2 vertical profile retrieval from SCIAMACHY limb measurements.

consideration with respect to the information content of SCIAMACHY limb measurements follows then looking at the averaging kernels. Between 18 and 35 km the averaging kernels reach a value of 1.0 at their maxima indicating a complete independence of the retrieved profile from a priori information. Due to a decreasing information content of the measurements and, thus, increasing dependence of the retrieved NO_2 amounts on a priori information and on NO_2 amounts at the neighboring altitude levels, the averaging kernels become wider and have lower maximum values above and below. For example, looking at the averaging kernel peaking at 12 km one see that the contribution of the true atmospheric state at this altitude to the retrieved NO_2 amount is only as high as 45% and the remaining information is originated from upper and lower neighboring altitude levels (by about 15% each) and a priori knowledge. As seen from the right plot in Fig. 4, the weighting functions have pronounced maxima near the tangent height only at tangent heights above 20 km. At lower tangent heights, weighing functions become wider and have a smooth maxima between 20 and 30 km indicating that most of the spectral signal is originating from the higher altitudes rather than from the tangent point region. Nevertheless, down to 12 km the weighting functions at different tangent heights have different shapes allowing the NO_2 amounts below 20 km to be retrieved.

Fig. 5 shows the theoretical precision (left plot), averaging kernels (middle plot), and differential weighting functions at 338.6 nm (right plot) for BrO vertical profile retrieval from SCIAMACHY limb measurements. The results were obtained using the limb measurement at a tangent height of 38.5 km as a reference spectrum. Similar to NO_2, the theoretical precision of the BrO vertical profile retrieval is about 10–20% in the altitude region 18–28 km decreasing to 20–40% above 28 km and between 14 and 18 km rapidly degrading below 14 km. The peak values of the averaging kernels are close to 1.0 only between 18 and 25 km decreasing to 0.9–0.95 above 25 km and between 14 and 18 km. The peak value of about 0.55 at 12 km altitude indicates an increased dependence of the retrieved BrO amount at this altitude on BrO amount at neighboring altitude levels and a priori information. Looking at the right plot in Fig. 5 one sees that down to 18 km tangent height the weighting functions exhibit relatively sharp peaks near the tangent height, whereas at all tangent heights below 18 km the weighting functions peak at about 18 km altitude. Nevertheless, similar to NO_2, the BrO amounts down to 12 km can be retrieved due to different shapes of the corresponding weighting functions.

Further investigations of the sensitivity of NO_2 and BrO vertical profile retrieval were performed using a numerical modeling of the measured data, i.e., a set of limb measurements at different tangent heights was simulated using the forward model assuming a certain state of the atmosphere denoted below as "true". Thereafter the retrieval was performed considering this set of simulated limb spectra as a real measurement sequence.

Fig. 6 shows a set of NO_2 vertical profiles retrieved assuming diverse a priori profiles as well as corresponding relative differences between retrieved and true profiles. As clearly seen, the differences are within 10% down to 18 km increasing to 30–40% at 12 km. Thus, in conformance with the conclusions following from theoretical sensitivity investigations above, a substantial influence of a priori information on the retrieved values is observed below 15 km only. Fig. 7 illustrates the dependence of the BrO vertical profile retrieval on a

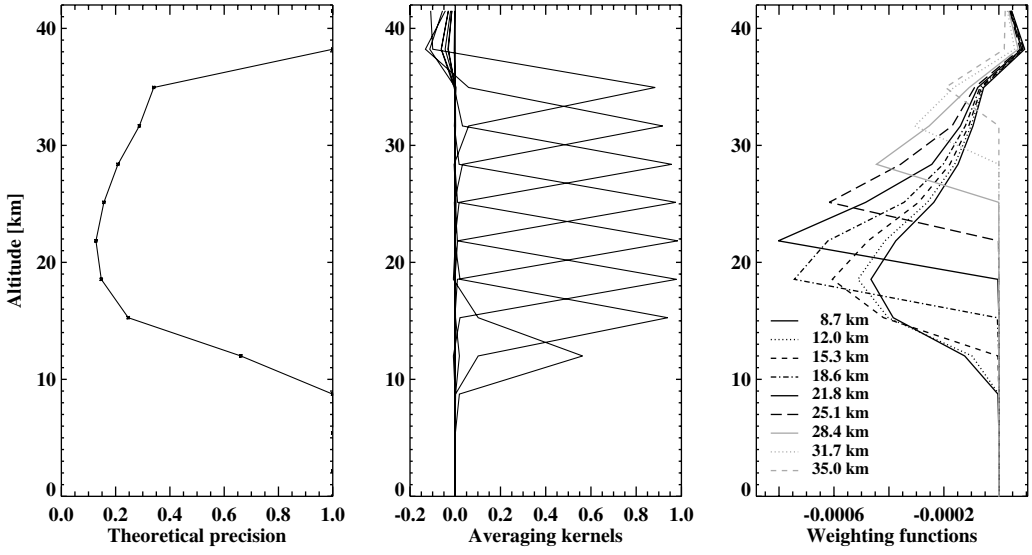

Fig. 5. Theoretical precision (left plot), averaging kernels (middle plot), and differential weighting functions at 338.6 nm (right plot) for BrO vertical profile retrieval from SCIAMACHY limb measurements.

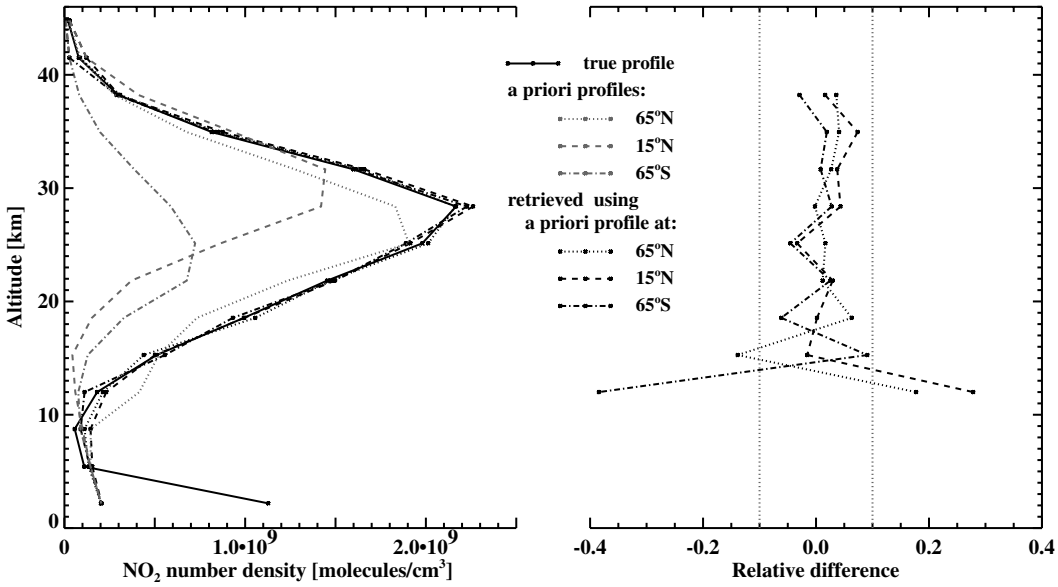

Fig. 6. Sensitivity of NO_2 vertical profile retrieval to a priori information. Left plot: true, a priori, and retrieved profiles of NO_2. Right plot: relative deviation of the NO_2 vertical profiles retrieved assuming different a priori profiles with respect to true profile.

priori information in the same manner as Fig. 6 for NO_2. Similar to NO_2, there is no significant dependence on a priori information down to 15 km.

Fig. 8 illustrates the sensitivity of NO_2 vertical profile retrieval to the pressure and temperature profiles employed in the forward model. The limb measurement sequence was simulated using the temperature profile marked as "true" then retrieved using in the forward model climatological pressure and temperature profiles appropriate to different latitude regions and NO_2 profile appropriate to 65°N (as shown in Fig. 6). The sensitivity of the NO_2 vertical profile retrieval to the temperature profile is mainly caused by the temperature dependence of NO_2 cross-sections employed in the forward model. Above 20 km, retrieved vertical profiles of NO_2 are almost independent of the pressure and temperature profiles used in the forward model. At lower altitudes, however, this dependence becomes stronger resulting in relative differences between retrieved and true profiles up to 80%.

Fig. 9 illustrates the sensitivity of BrO vertical profile retrieval to the pressure and temperature profiles employed in the forward model. Similar to NO_2, the limb measurement sequence was simulated using the temperature profile marked as "true" and then retrieved using in the forward model climatological pressure and

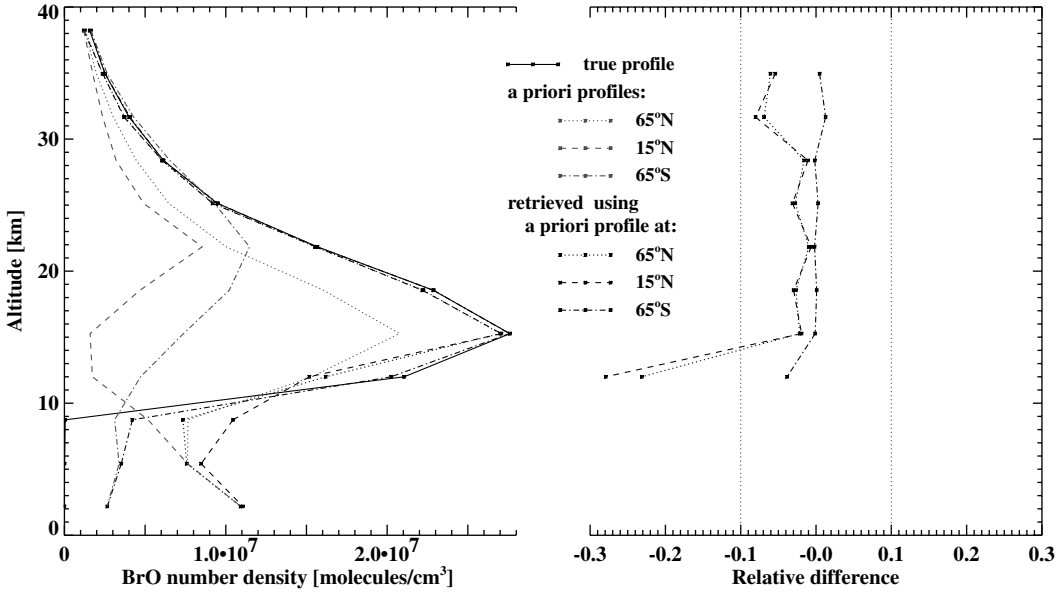

Fig. 7. Sensitivity of BrO vertical profile retrieval to a priori information. Left plot: true, a priori, and retrieved profiles of BrO. Right plot: relative deviation of the BrO vertical profiles retrieved assuming different a priori profiles with respect to true profile.

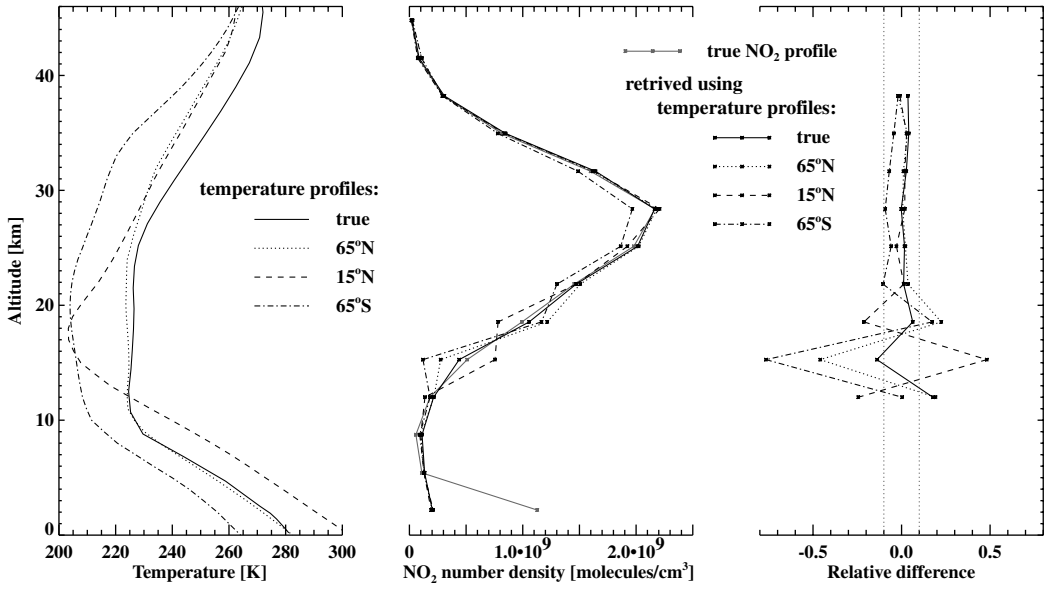

Fig. 8. Sensitivity of NO_2 vertical profile retrieval to the pressure and temperature profiles (climatological profiles in different latitude regions in August). Left plot: temperature profiles used in the forward model. Middle plot: true (gray curve) and retrieved (black curves) profiles of NO_2. Right plot: relative deviation of the NO_2 vertical profiles retrieved using different pressure and temperature profiles with respect to the true profile.

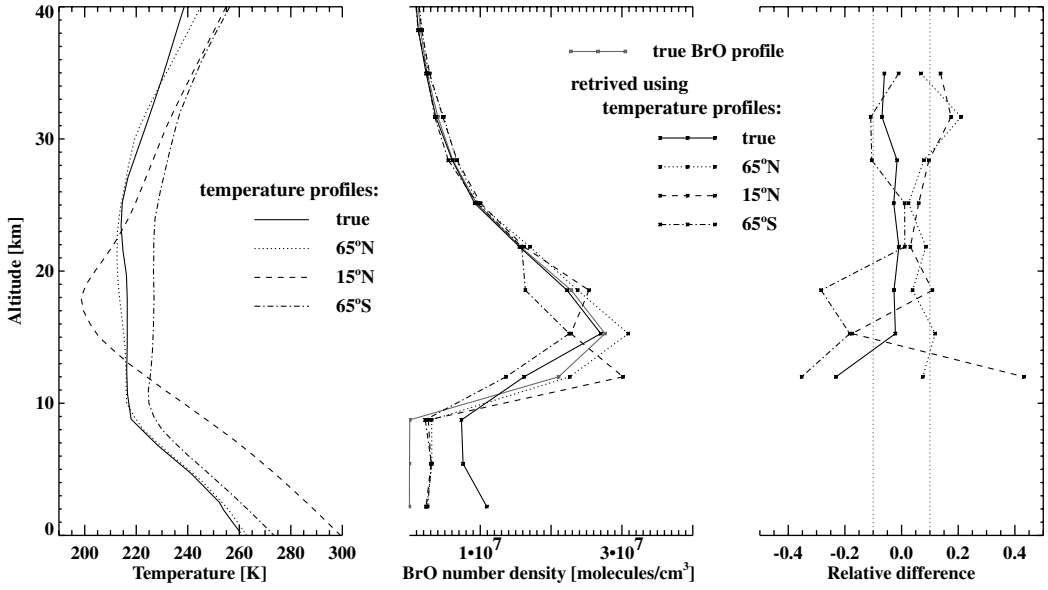

Fig. 9. Sensitivity of BrO vertical profile retrieval to the pressure and temperature profiles (climatological profiles in different latitude regions in February). Left plot: temperature profiles used in the forward model. Middle plot: true (gray curve) and retrieved (black curves) profiles of BrO. Right plot: relative deviation of the BrO vertical profiles retrieved using different pressure and temperature profiles with respect to the true profile.

temperature profiles appropriate to different latitude regions and BrO profile appropriate to 65°N (as shown in Fig. 7). The sensitivity of the BrO vertical profile retrieval to the temperature profile is mainly caused by the temperature dependence of ozone cross-sections employed in the forward model. As seen from the plot, the dependence on the pressure and temperature is insignificant between 20 and 30 km increasing to 20–30% above 30 km and between 15 and 20 km. A much stronger influence of the pressure and temperature profiles used in the forward model is observed below 15 km resulting in relative differences between retrieved and true profiles up to 50%.

4. Conclusions

A retrieval algorithm employed to obtain vertical distributions of NO_2 and BrO from SCIAMACHY limb measurements was discussed. Comparisons of atmo-

spheric trace gas vertical distributions retrieved from SCIAMACHY limb measurements with the results obtained by other instruments show a reasonable agreement.

The sensitivity region is estimated to be 12–40 km for NO_2 and 12–35 km for BrO. Above 15 km, there is no significant dependence of the retrieved profiles on a priori information for both NO_2 and BrO, whereas major retrieval problems are expected below associated to the increasing influence of the information originating from the upper and lower neighboring altitude levels as well as form a priori knowledge.

The dependence of the retrieved trace gas vertical distributions on the pressure and temperature profiles used in the forward model is insignificant above 20 km, whereas it cannot be completely ignored when retrieving the trace gas amounts below. However, it should be pointed out that very strong changes in the vertical profiles of pressure and temperature used in the forward simulations result in moderate errors in the retrieved profiles. Thus, using realistic pressure and temperature distributions, for example, from ECMWF database, the retrieval error can be minimized.

Acknowledgements

This work has been funded in parts by the German Ministry of Education and Research BMBF (Grant 07UFE12/8), the German Aerospace Center DLR (Grant 50EE0027), and the European Union (project TOPOZ-III, EVK2-CT-2001-00102). Some data shown here were calculated on HLRN (High-Performance Computer Center North). Services and support are gratefully acknowledged.

References

Bovensmann, H., Burrows, J.P., Buchwitz, M., Frerick, J., Noël, S., Rozanov, V.V. SCIAMACHY: mission objectives and measurement modes. J. Atmos. Sci. 56 (2), 127–149, 1999.

Bovensmann, H., Buchwitz, M., Frerick, J., Hoogeveen, R., Kleipool, Q., Lichtenberg, G., Noël, S., Richter, A., Rozanov, A., Rozanov, V.V., Skupin, J., von Savigny, C., Wuttke, M., Burrows, J.P. SCIAMACHY on ENVISAT: in-flight optical performance and first results, in: Schäfer, K.P., Comeron, A., Carleer, M.R., Picard, R.H. (Eds.), Remote Sensing of Clouds and the Atmosphere VIII Proceedings of SPIE 5235, pp. 160–173, 2004.

Bracher, A., Sinnhuber, M., Rozanov, A., Burrows, J.P. Using a photochemical model for the validation of NO_2 satellite measurements at different solar zenith angles. Atmos. Chem. Phys. 5, 393–408, 2005.

Haley, C.S., Brohede, S.M., Sioris, C.E., Griffioen, E., Murtagh, D.P., McDade, I.C., Eriksson, P., Llewellyn, E.J., Bazureau, A., Goutail, F. Retrieval of stratospheric O_3 and NO_2profiles from Odin Optical Spectrograph and Infrared Imager System (OSIRIS) limb-scattered sunlight measurements. J. Geophys. Res. 109, D16303, 2004.

Hoogen, R., Rozanov, V.V., Burrows, J.P. Ozone profiles from GOME satellite data: algorithm description and first validation. J. Geophys. Res. 104, 8263–8280, 1999.

Kaiser, J.W., von Savigny, C., Eichmann, K.-U., Noël, S., Bovensmann, H., Frerick, J., Burrows, J.P. Pointing retrieval from limb scattering observations by SCIAMACHY. Can. J. Phys. 82 (12), 1041–1052, 2004.

Loughman, R.P., Griffioen, E., Oikarinen, L., Postylyakov, O.V., Rozanov, A., Flittner, D.E., Rault, D.F. Comparison of radiative transfer models for limb-viewing scattered sunlight measurements. J. Geophys. Res. 109, 2004.

Mauldin, L.E., Zaun, N.H., McCormick, M.P., Guy, J.J., Vaughn, W.R. Stratospheric aerosol and gas experiment II instrument: a functional description. Opt. Eng. 24, 307, 1985.

Mount, G.H., Rusch, D.W., Noxon, J.F., Zawodny, J.M., Barth, C.A. Measurements of stratospheric NO_2 from the Solar Mesosphere Explorer satellite: 1. An overview of the results. J. Geophys. Res. 89, 1327–1340, 1984.

Postylyakov, O.V. Radiative transfer model MCC++ with evaluation of weighting functions in spherical atmosphere for use in retrieval algorithms. Adv. Space Res. 34, 721–726, 2004.

Rodgers, C.D. Inverse Methods for Atmospheric Sounding: Theory and Practice. World Scientific, Singapore, 2000.

Rozanov, A., Rozanov, V., Burrows, J.P. A numerical radiative transfer model for a spherical planetary atmosphere: combined differential–integral approach involving the Picard iterative approximation. J. Quant. Spectrosc. Radiat. Transfer 69, 513–534, 2001.

Russel III, J.M., Gordley, L.L., Gordley, J.H., Park, J.H., Drayson, S.R., Hesketh, W.D., Cicerone, R.J., Tuck, A.F., Frederick, J.E., Harries, J.E., Crutzen, P.J. The halogen occultation experiment. J. Geophys. Res. 98, 10777–10797, 1993.

von Savigny, C., Rozanov, A., Bovensmann, H., Eichmann, K.-U., Noel, S., Rozanov, V.V., Sinnhuber, B.-M., Weber, M., Burrows, J.P. The ozone hole break-up in September 2002 as seen by SCIAMACHY on ENVISAT. J. Atmos. Sci. (in press) 2005.

Sioris, C.E., Haley, C.S., McLinden, C.A., von Savigny, C., McDade, I.C., McConnell, J.C., Evans, W.F.J., Lloyd, N.D., Llewellyn, E.J., Chance, K.V., Kurosu, T.P., Murtagh, D., Frisk, U., Pfeilsticker, K., Boesch, H., Weidner, F., Strong, K., Stegman, J., Megie, G. Stratospheric profiles of nitrogen dioxide observed by Optical Spectrograph and Infrared Imager System on the Odin satellite. J. Geophys. Res. 108, 2003.